On the Performance of Multi-Robot Wireless-Based Networks

Van Son NGUYEN [1], Trinh Van CHIEN [2], Dang Khanh HOA [1], Do Dinh HUNG [1], Hoai Giang NGUYEN [1], Chi Quynh LE [3], Lam-Thanh TU [4,]*

[1] Faculty of Electrical and Electronic Engineering, Hanoi Open University, 100000 Hanoi, Vietnam
[2] School of Information and Communication Technology (SoICT), Hanoi University of Science and Technology (HUST), 100000 Hanoi, Vietnam
[3] Electric Power University, 100000 Hanoi, Vietnam
[4] Communication and Signal Processing Research Group, Faculty of Electrical and Electronics Engineering, Ton Duc Thang University, Ho Chi Minh City, 70000 Vietnam

tulamthanh@tdtu.edu.vn*

Submitted July 2, 2023 / Accepted December 8, 2023 / Online first December 21, 2023

Abstract. *The performance of the multi-robot wireless-based networks is investigated in this paper. Particularly, we derive the outage probability (OP) and potential throughput (PT) of the worst terminal in the closed-form expressions under two scenarios, with and without direct transmission from the centre robot to all terminal robots. The considered system is complicated since it involves many random variables (RVs) and they are correlated owing to the common link from the central robot to the relay one. To overcome such correlations, our approach is to first derive the performance of the considered metric condition on the correlated link, we then take the average over the common link. Numerical results based on the Monte-Carlo method are given to verify the accuracy of the derived framework as well as to identify the behaviors of two metrics with respect to some key parameters such as the transmit power at both central and immediate robots.*

Keywords

Multi-robot networks, outage probability, selection combining, performance analysis, potential throughput

1. Introduction

Multi-robot wireless-based networks (MWN) is the smart combination of multi-robot networks (RNs) and wireless networks (WNs) that inherits the advantages from both sides [1]. Particularly, robots are generally employed to do tasks that are not able to handle by humans, i.e., entering risky areas such as high radiation areas. However, a single robot can not generally tackle these tasks efficiently and quickly. As a consequence, multi-robot networks are deployed in practice to facilitate performance. In order to communicate between robots and robots or centre robots, wireless communications is a wise and efficient choice since it can be employed in any places even the disaster areas. Additionally, multi-robot networks with wireless communications capabilities can also improve reliability and scalability. Here, reliability refers to a case where one robot suddenly gets malfunctions, other robots can complement its tasks to achieve the whole target. Scalability is more obvious since with a large number of robots one can enhance the working area. Nonetheless, these advantages rely on the assumption that error-free communications between these robots are available. It, however, is not a case in practical scenarios such as under the harsh weather, environments, etc. As a consequence, the present work focuses on the improvement of communications in multi-robot networks. Particularly, we consider an MWN where some immediate robots can help the sink node to forward vital information to all end-robot. Before going to highlight the main contributions and novelties of the paper. Let us shortly summarize some state-of-the-art in MWN.

The performance of MWN was studied widely in [2–8]. Particularly, communications between two swarm robots were supported by employing unmanned aerial vehicles (UAVs). The results unveiled that by optimally allocating transmit power and UAV's trajectory, the sum rate of the system is improved significantly. These findings, however, count on numerical results rather than on the rigorous mathematical framework. Improving the coverage area of the multiple mobile robot networks was addressed in [3] with the help of reinforcement learning (RL). They, nonetheless, focus on extending the coverage area instead of facilitating the reliability of the WRN. A novel protocol named LEACH-R to relay information in mobile swarm robots was proposed in [5]. They showed that their proposed scheme outperforms another in terms of packet delivery ratio, and probability of interruption of network links. The design and simulation of multi-robot systems deploying Zigbee were conducted in [6].

DOI: 10.13164/re.2024.0127

Okonkwo and others in [7] studied time-varying ultra-wideband (UWA) channel modeling of robot-to-robot communications. They found that in the case non light-of-sight (NLOS) scenario, the stationary bandwidth depends on the proximity and distribution of the scatters. The performance of a multi-robot rescue system communicated by an ad hoc network was studied in [8].

Different from the above-mentioned work, in the present paper, we study the communications performance of the multi-robot wireless-based networks where a central robot sends command tasks to all terminal robots with the help of a relay robot. Some practical scenarios of the considered system are the following: the central robot sends commands to all robots to rescue/help people, perform relief activities in the disaster areas or enter the dangerous area to perform some special tasks, i.e., removing radiated waste, etc. More precisely, we derive in closed-form expressions the outage probability (OP) and the potential throughput (PT) of the worst robot under two scenarios, with and without direct transmission from the central robot to all terminal robots. The main contributions and novelties of the present paper are summarized as follows:

- To the best of the authors' knowledge, we are a pioneer to study the performance of the multi-robot wireless-based networks. The considered system is highly complicated with involves many correlated random variables (RVs).
- As the performance of the whole systems is bottleneck at the worst end-robot, we thus derive in closed-form expressions the OP and PT of the worst terminal robots under two cases, with and without direct link from source to destination robots.
- We provide numerical results to verify the correctness of the derived mathematical framework and to highlight the behaviors of two considered metrics under the impact of some vital parameters such as the transmit power at the centre and relay robots.

The remainder of the manuscript is organized as follows: Section 2 provides the system model. The main derivations and trends are given in Sec. 3. Numerical results are provided in Sec. 4. Section 5 concludes the main observations from the paper.

2. System Model

We consider a wireless-based multi-robot system where a sink node denoted by S wants to broadcast information to $\mathcal{N}$ robots denoted by D_n, $n \in \{1, \ldots, \mathcal{N}\}$ with the help of an immediate robot between S and all D as illustrated in Fig. 1. It is noted that the relay robot is generally located in the middle between the central and terminal robots. Additionally, we consider a case where each robot is equipped with only a single antenna, the multi-antenna case is left for future work.

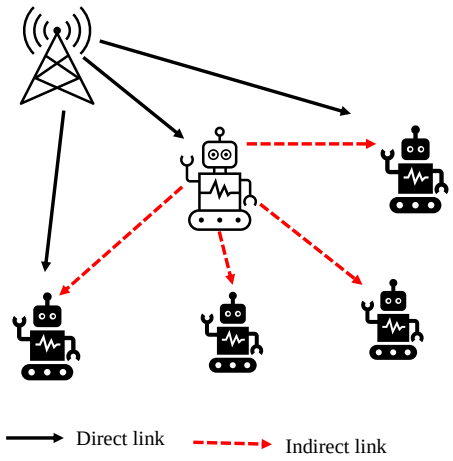

Fig. 1. The considered multi-robot wireless-based networks.

2.1 Transmission Procedure

We consider two scenarios in the present work. In the first case denoted by (C1), we assume that the direct transmission between the commander and terminal robots are not existed owing to deep fading and obstacles [9]. In the second case denoted by (C2), the direct link between S and D_n, $n \in \{1, \ldots \mathcal{N}\}$ exists. In both cases, the whole transmission takes place in two consecutive time slots/phases. In the first phase, the centre robot sends information to the immediate robot (C1) or all robots in the networks (C2). At the end of the first phase, the relay robot will decode this information. Next, in the second phase, it will re-encode and forward the source information to all destination robots. It is emphasized that the considered protocol overcomes the popular issue of amplify-and-forward (AF) protocol that the immediate robot amplifies both useful signals plus noise and forwards to the destinations. For the second case (C2), each terminal robot will employ the selection combining (SC) technique to combine information from the source and relay robots.

2.2 Channel Modelling

All wireless links in the considered multi-robot networks are subjected to both small-scale fading and large-scale path loss. which are practical. The impact of the shadowing is not taken into account as it is a favored case in the literature for short-range communications [10].

Small-Scale Fading Let us denote $c_{a,b}$, $a \in \{\mathrm{S}, \mathrm{R}\}$, $b \in \{\mathrm{R}, \mathrm{D}_n\}$, $n \in \{1, \ldots, \mathcal{N}\}$, as the channel coefficient between transmitter a and receiver b that is modeled by a complex Gaussian distribution with zero mean and α variance, i.e., $\mathcal{CN}(0, \alpha)$. As a consequence, the channel gain between node a and b denoted by $g_{a,b} = \left|c_{a,b}\right|^2$ is followed by an exponential distribution with scale parameter α. It is noted that the adopted fading modeling provides the worst performance compared with other fading distributions thus, the considered system can work well in any practice environ-

ment. Moreover, we assume that fading is fixed in one-time slot and changes independently between time slots.

Large-Scale Path-Loss Let us denote $l_{a,b}$ as the large-scale path-loss from robot a to robot b, it is then defined as follows [11]:

$$l_{a,b} = L_0\big(\max\left(1, d_{a,b}\right)\big)^{\chi} \tag{1}$$

where χ and $L_0 = \left(\frac{4\pi}{\lambda}\right)^2$ are the path-loss exponent and the path-loss constant, $d_{a,b}$ is the transmission distance from $a \to b$, $\lambda = \frac{c}{f_c}$ is the wavelength, c (in m/s) is the speed of light, and f_c (in Hz) is the carrier frequency.

Remark 1 *It should be noted that the adopted large-scale path-loss model overcomes the popular issue of the unbounded path-loss model that the receiver power at the receiver approaches infinity when the transmission distance reaches zero [12].*

2.3 Signal-to-Noise Ratio (SNR)

The received signals at the relay robot and the n-th terminal robot from S at the first phase denoted by y_{R} and $y_{\mathrm{S},n}$, $n \in \{1, \ldots, \mathcal{N}\}$ are formulated as follows:

$$\begin{aligned} y_{\mathrm{R}} &= \sqrt{P_{\mathrm{S}} l_{\mathrm{S,R}}^{-1}} c_{\mathrm{S,R}} x_{\mathrm{S}} + n_{\mathrm{R}}, \\ y_{\mathrm{S},n} &= \sqrt{P_{\mathrm{S}} l_{\mathrm{S},n}^{-1}} c_{\mathrm{S},n} x_{\mathrm{S}} + n_n^1, \quad \forall n \end{aligned} \tag{2}$$

where P_{S} is the transmit power of the central robot; x_{S} is the transmitted signals of the central robot with $\mathbb{E}\left\{|x_{\mathrm{S}}|^2\right\} = 1$, $\mathbb{E}\{\cdot\}$ is the expectation operator. n_{R} and n_n are the additive Gaussian white noise (AWGN) at relay and n-th robot with zero mean and variance $\sigma_{\mathrm{R}}^2 = \sigma_n^2 = \sigma^2 = -174 + NF + 10\log(BW), \forall n$ [13]; where NF (in dB) is the noise figure; and BW (in Hz) is the transmission bandwidth. The received signals at the n-th terminal robot at the 2nd phase are computed as

$$y_{\mathrm{R},n} = \sqrt{P_{\mathrm{R}} l_{\mathrm{R},n}^{-1}} c_{\mathrm{R},n} x_{\mathrm{R}} + n_n^2, \quad \forall n. \tag{3}$$

Here P_{R} is the transmit power of the relay robot. From (2) and (3), the signal-to-noise ratio (SNR) of the indirect link from source to the n-th robot via relay robot denoted by γ_n^{I} is formulated as [14]:

$$\gamma_n^{\mathrm{I}} = \min\left\{\frac{P_{\mathrm{S}} l_{\mathrm{S,R}}^{-1}\left|c_{\mathrm{S,R}}\right|^2}{\sigma^2}, \frac{P_{\mathrm{R}} l_{\mathrm{R},n}^{-1}\left|c_{\mathrm{R},n}\right|^2}{\sigma^2}\right\}, \quad \forall n \tag{4}$$

where $\min\{\cdot,\cdot\}$ is the minimum function. It is noted that if the first scheme is taken into account, the end-to-end (e2e) SNR is exactly the same as $\gamma_n^{\mathrm{I}} = \gamma_n^{\mathrm{e2e,C1}}$. On the other hand, if the second scheme (considering the direct link) is employed, the e2e SNR at the n-th robot is computed as [15]:

$$\gamma_n^{\mathrm{e2e,C2}} = \max\left\{\frac{P_{\mathrm{S}} l_{\mathrm{S},n}^{-1}\left|c_{\mathrm{S},n}\right|^2}{\sigma^2}, \gamma_n^{\mathrm{e2e,C1}}\right\}. \tag{5}$$

Remark 2 *It is no doubt to point out that the e2e SNR of the 2nd scheme includes the e2e SNR of the first scheme. Thus, it is certain that the performance of the 2nd scheme always outperforms another.*

In the present work, we investigate the performance of the worst robot. From (5) and (4), the e2e SNR of the worst destination under the 1st and 2nd scheme denoted by γ_{w}^{e}, $e \in \{\mathrm{C1}, \mathrm{C2}\}$ is given as

$$\begin{aligned} \gamma_{\mathrm{w}}^{\mathrm{C2}} &= \min_{n\in\{1,N\}}\left\{\gamma_n^{\mathrm{e2e,C2}}\right\} \\ &= \min_{n\in\{1,N\}}\left\{\max\left\{\frac{P_{\mathrm{S}}\left|c_{\mathrm{S},n}\right|^2}{l_{\mathrm{S},n}\sigma^2}, \min\left\{\frac{P_{\mathrm{S}}\left|c_{\mathrm{S,R}}\right|^2}{l_{\mathrm{S,R}}\sigma^2}, \frac{P_{\mathrm{R}}\left|c_{\mathrm{R},n}\right|^2}{l_{\mathrm{R},n}\sigma^2}\right\}\right\}\right\}, \\ \gamma_{\mathrm{w}}^{\mathrm{C1}} &= \min_{n\in\{1,N\}}\left\{\gamma_n^{\mathrm{e2e,C1}}\right\} \\ &= \min_{n\in\{1,N\}}\left\{\min\left\{\frac{P_{\mathrm{S}}\left|c_{\mathrm{S,R}}\right|^2}{l_{\mathrm{S,R}}\sigma^2}, \frac{P_{\mathrm{R}}\left|c_{\mathrm{R},n}\right|^2}{l_{\mathrm{R},n}\sigma^2}\right\}\right\}. \end{aligned} \tag{6}$$

Remark 3 *Direct inspection (6), we observe that the e2e SNR of all terminal robots is not independent of each other since all e2e SNR rely on the SNR of the 1st hop from the centre to the relay robot. As a consequence, the derivation of the considered system is extremely difficult for an arbitrary number of terminal robots.*

In the next section, we are going to address the performance of two considered metrics which are outage probability and potential throughput.

3. Performance Analysis

In this section, we investigate the outage probability and the potential throughput of the worst robots under two schemes [12]. Let us first study the OP and followed by the PT.

3.1 Outage Probability

3.1.1 Outage Probability of the Worst Robot under the 1st Scheme

The outage probability of the robot under the first scheme is computed as

$$\begin{aligned} \mathrm{OP}^{\mathrm{C1}} &= \Pr\left\{\gamma_{\mathrm{w}}^{\mathrm{C1}} \le \gamma_{\mathrm{th}}\right\} \\ &= \Pr\left\{\min_{n\in\{1,N\}}\left\{\min\left\{\left|c_{\mathrm{S,R}}\right|^2\frac{P_{\mathrm{S}}}{l_{\mathrm{S,R}}\sigma^2}, \frac{P_{\mathrm{R}}}{l_{\mathrm{R},n}\sigma^2}\left|c_{\mathrm{R},n}\right|^2\right\}\right\} \le \gamma_{\mathrm{th}}\right\} \\ &\overset{(a)}{=} \Pr\left\{\min\left\{\left|c_{\mathrm{S,R}}\right|^2\frac{P_{\mathrm{S}}}{l_{\mathrm{S,R}}\sigma^2}, \frac{P_{\mathrm{R}}}{l_{\mathrm{R},n}\sigma^2}\min_{n\in\{1,N\}}\left\{\left|c_{\mathrm{R},n}\right|^2\right\}\right\} \le \gamma_{\mathrm{th}}\right\} \\ &\overset{(b)}{=} 1 - \overline{F}_{|c_{\mathrm{S,R}}|^2}\left(\gamma_{\mathrm{th}}\frac{l_{\mathrm{S,R}}\sigma^2}{P_{\mathrm{S}}}\right)\overline{F}_{U=\min\limits_{n\in\{1,N\}}\left\{|c_{\mathrm{R},n}|^2\right\}}\left(\gamma_{\mathrm{th}}\frac{l_{\mathrm{R},n}\sigma^2}{P_{\mathrm{R}}}\right) \\ &\overset{(c)}{=} 1 - \exp\left(-\gamma_{\mathrm{th}}\frac{l_{\mathrm{S,R}}\sigma^2}{P_{\mathrm{S}}\alpha_{|c_{\mathrm{S,R}}|^2}}\right)\left(\prod_{n=1}^{N}\left(\exp\left(-\gamma_{\mathrm{th}}\frac{l_{\mathrm{R},n}\sigma^2}{P_{\mathrm{R}}\alpha_{|c_{\mathrm{R},n}|^2}}\right)\right)\right) \end{aligned} \tag{7}$$

where $\gamma_{\text{th}} = 2^{2R} - 1$, R (in bits/s/Hz) is the expected rate, (a) is attained by exploiting the property that minimizing the e2e SNR of dual-hop SNR is equivalent to minimizing the 2nd hop, i.e., from relay to terminals, since all links utilize the same first hop, e.g., from centre to relay robot, (b) is held by using the independent property between the 1st and 2nd hop and the order statistic, and (c) is obtained by substituting the CDF of the exponential RV and the minimum of the independent and non-identically distributed (i.n.i.d.) exponential RVs.

3.1.2 Outage Probability of the Worst Robot under the 2nd Scheme

Different from the 1st scheme where the direct link does not take into account. In the 2nd scheme, the direct link exists and has a countable contribution to the e2e SNR. It, as a result, improves the system's performance. However, from the mathematical framework point of view, it is more challenging. More precisely, we can not employ the equivalent property in (7) because there is a maximum function between two minimum functions of $\gamma_{\text{w}}^{\text{C2}}$ in (6). Thus, we need to deploy another technique in order to derive the OP in the closed-form expression. Particularly, we first compute the OP of the worst robot condition on the channel gain from the centre robot to the immediate robot denoted by OP_X^{C2} and is formulated as follows:

$$\begin{aligned}\text{OP}_X^{\text{C2}} &= \Pr\left\{\gamma_{\text{w}}^{\text{C2}} \le \gamma_{\text{th}} \middle| X = \left|c_{\text{S,R}}\right|^2\right\} \\ &= \Pr\left\{\min_{n\in\{1,N\}}\left\{\max\left\{\frac{P_{\text{S}}\left|c_{\text{S},n}\right|^2}{l_{\text{S},n}\sigma^2},\right.\right.\right. \\ &\quad \left.\left.\left.\min\left\{\frac{P_{\text{S}}X}{l_{\text{S,R}}\sigma^2}, \frac{P_{\text{R}}\left|c_{\text{R},n}\right|^2}{l_{\text{R},n}\sigma^2}\right\}\right\}\right\} \le \gamma_{\text{th}}\right\}. \end{aligned} \tag{8}$$

To compute the probability in (8) let us define a random variable Z_n conditions on X as $Z_n = \frac{P_{\text{S}}}{l_{\text{S,R}}\sigma^2}\min\left\{X, \frac{P_{\text{R}}l_{\text{S,R}}}{P_{\text{S}}l_{\text{R},n}}\left|c_{\text{R},n}\right|^2\right\}$ [16]. Its cumulative distribution function (CDF) is then computed as follows:

$$\begin{aligned} F_{Z_n}(z;x) &= \Pr\{Z_n \le z\} \\ &= \Pr\left\{\frac{P_{\text{S}}}{l_{\text{S,R}}\sigma^2}\min\left\{X, \frac{P_{\text{R}}l_{\text{S,R}}}{P_{\text{S}}l_{\text{R},n}}\left|c_{\text{R},n}\right|^2\right\} \le z\right\} \\ &= \Pr\left\{\frac{P_{\text{R}}l_{\text{S,R}}}{P_{\text{S}}l_{\text{R},n}}\left|c_{\text{R},n}\right|^2 < z\frac{l_{\text{S,R}}\sigma^2}{P_{\text{S}}}, \frac{P_{\text{R}}l_{\text{S,R}}}{P_{\text{S}}l_{\text{R},n}}\left|c_{\text{R},n}\right|^2 < x\right\} \\ &\quad + \Pr\left\{x < z\frac{l_{\text{S,R}}\sigma^2}{P_{\text{S}}}, \frac{P_{\text{R}}l_{\text{S,R}}}{P_{\text{S}}l_{\text{R},n}}\left|c_{\text{R},n}\right|^2 \ge x\right\} \\ &= \Pr\left\{\frac{P_{\text{R}}l_{\text{S,R}}}{P_{\text{S}}l_{\text{R},n}}\left|c_{\text{R},n}\right|^2 < \min\left(x, z\frac{l_{\text{S,R}}\sigma^2}{P_{\text{S}}}\right)\right\} \\ &\quad + \Pr\left\{\left|c_{\text{R},n}\right|^2 > x\frac{P_{\text{S}}l_{\text{R},n}}{P_{\text{R}}l_{\text{S,R}}}\right\}\text{H}\left(z\frac{l_{\text{S,R}}\sigma^2}{P_{\text{S}}} - x\right) \\ &= 1 - \exp\left(-\frac{P_{\text{S}}l_{\text{R},n}}{\alpha_{\left|c_{\text{R},n}\right|^2}P_{\text{R}}l_{\text{S,R}}}\min\left(x, z\frac{l_{\text{S,R}}\sigma^2}{P_{\text{S}}}\right)\right) \\ &\quad + \exp\left(-\frac{x}{\alpha_{\left|c_{\text{R},n}\right|^2}}\frac{P_{\text{S}}l_{\text{R},n}}{P_{\text{R}}l_{\text{S,R}}}\right)\text{H}\left(z\frac{l_{\text{S,R}}\sigma^2}{P_{\text{S}}} - x\right) \end{aligned} \tag{9}$$

where $\text{H}(\cdot)$ is the Heaviside function. Having obtained the CDF of Z_n, the CDF of the e2e SNR of the n-th terminal robot condition on X is given as follows:

$$\begin{aligned} F_{\gamma_n^{\text{e2e,C2}}\left|X\right.}(w) &\overset{(a)}{=} F_{\left|c_{\text{S},n}\right|^2}\left(w\frac{l_{\text{S},n}\sigma^2}{P_{\text{S}}}\right)F_{Z_n}(w;x) \\ &\overset{(b)}{=} \left(1 - \exp\left(-\frac{wl_{\text{S},n}\sigma^2}{P_{\text{S}}\alpha_{\left|c_{\text{S},n}\right|^2}}\right)\right) \\ &\quad \times\left(1 - \exp\left(-\frac{P_{\text{S}}l_{\text{R},n}}{\alpha_{\left|c_{\text{R},n}\right|^2}P_{\text{R}}l_{\text{S,R}}}\min\left(x, w\frac{l_{\text{S,R}}\sigma^2}{P_{\text{S}}}\right)\right)\right) \\ &\quad + \exp\left(-\frac{x}{\alpha_{\left|c_{\text{R},n}\right|^2}}\frac{P_{\text{S}}l_{\text{R},n}}{P_{\text{R}}l_{\text{S,R}}}\right)\text{H}\left(w\frac{l_{\text{S,R}}\sigma^2}{P_{\text{S}}} - x\right)\Bigg) \end{aligned} \tag{10}$$

where (a) is attained by employing the independent property between the direct and indirect links and (b) is held by substituting the CDF of the exponential random variable and (9). The CDF of OP_X^{C2} is then calculated as

$$\begin{aligned} \text{OP}_X^{\text{C2}}(R;x) &= \Pr\left\{\gamma_{\text{w}}^{\text{C2}} \le R\middle| X = \left|c_{\text{S,R}}\right|^2\right\} \\ &= \Pr\left\{\min_{n\in\{1,N\}}\left\{\gamma_n^{\text{e2e,C2}}\middle| X\right\} \le \gamma_{\text{th}}\right\} \\ &= 1 - \Pr\left\{\max_{n\in\{1,N\}}\left\{\gamma_n^{\text{e2e,C2}}\middle| X\right\} \ge \gamma_{\text{th}}\right\} \\ &= 1 - \prod_{n=1}^{N}\overline{F}_{\gamma_n^{\text{e2e,C2}}\left|X\right.}(\gamma_{\text{th}}). \end{aligned} \tag{11}$$

Finally, by taking the average of the OP_X^{C2} over X, we obtain the OP of the worst robot as follows:

$$\begin{aligned} \text{OP}^{\text{C2}} &= \int_{x=0}^{\infty}\text{OP}_X^{\text{C2}}(R;x)\,f_{X=\left|c_{\text{S,R}}\right|^2}(x)\,\text{d}x \\ &= 1 - \left(\prod_{n=1}^{N}A_n\right)\left[\left(\prod_{n=1}^{N}\left[1 + C_n\right]\right)\exp\left(-\gamma_{\text{th}}\frac{l_{\text{S,R}}\sigma^2}{P_{\text{S}}\alpha_{\left|c_{\text{S,R}}\right|^2}}\right)\right. \\ &\quad \left. + \frac{1}{\alpha_{\left|c_{\text{S,R}}\right|^2}}\left(1 - \exp\left(-\gamma_{\text{th}}\frac{l_{\text{S,R}}\sigma^2}{P_{\text{S}}\alpha_{\left|c_{\text{S,R}}\right|^2}}\right)\right)\right]. \end{aligned} \tag{12}$$

Here $A_n = \exp\left(-\gamma_{\text{th}}\frac{\sigma^2 l_{\text{S},n}}{P_{\text{S}}\alpha_{\left|c_{\text{S},n}\right|^2}}\right)$,

$B_n = \exp\left(-\gamma_{\text{th}}\frac{\sigma^2 l_{\text{R},n}}{P_{\text{R}}\alpha_{\left|c_{\text{R},n}\right|^2}}\right)\left[1 - \exp\left(-\gamma_{\text{th}}\frac{\sigma^2 l_{\text{S},n}}{P_{\text{S}}\alpha_{\left|c_{\text{S},n}\right|^2}}\right)\right]$,

and $C_n = \frac{B_n}{A_n}$.

Proof: The proof is available in Appendix 1.

3.2 Potential Throughput

The potential throughput of the worst robot under the e-scheme is computed as follows:

$$\text{PT}^e = (1 - \text{OP}^e(\gamma_{\text{th}}))\log_2(1 + \gamma_{\text{th}}) \tag{13}$$

which measures the data rate that the network can provide to each robot and guarantees communication.

Remark 4 *This paper has investigated the two important measurement metrics for multi-robot wireless-based networks comprising the OP and potential throughput. Specifically, the OP indicates the probability of disconnection to each robot in the network under the quality of service requirements. Besides, the potential throughput defines the provided data rate to robots from the network.*

4. Numerical Results

In this section, we provide numerical results to verify the accuracy of the proposed mathematical framework versus Monte-Carlo simulations and to reveal the impact of some key parameters on the performance of both metrics, i.e., outage probability and potential throughput. Without loss of generality, the parameters are provided in Tab. 4. It is noted that the selected parameters have complied with current wireless networks. In particular, the selected carrier frequency and bandwidth are according to the 4G cellular networks [17]. The transmit power of P_{S} ranges from 0 to 40 dBm, with the default setting fixed at 20 dBm. The location of the central and relay robots are $(0, 0)$ [m] and $(40, 0)$ while the position of all terminal robots are following: $(80, 10)$, $(100, -20)$, $(80, 0)$, $(90, -10)$, respectively. All figures in this section are produced by using the popular software MATLAB[1] . Nonetheless, other popular open-source software like Python can also be considered to produce the below results. Regarding the hardware, the figures are mainly produced by the laptop Inspiron 13 5378 with the CPU Intel Core i7-7500 2.7 GHz and memory 16384 MB RAM.

Figure 2 illustrates the performance of both OP and PT versus R under two schemes. We first confirm that the derived mathematical framework matches well with simulation results via the Monte-Carlo method. Next, the performance of the 2nd scheme is better than the 1st scheme. Nonetheless, relying on the transmit power at both P_{S} and P_{R}, the gap can be indistinguishable or considerable. Particularly, if the transmit power at the center and relay robots are comparable, the performance of the two schemes is more or less the same, i.e., $P_{\mathrm{S}} = P_{\mathrm{R}} = 30$ dBm, and we observe a big gap if $P_{\mathrm{R}} \ll P_{\mathrm{S}}$. Besides, the OP is a monotonic increasing function with respect to R. It can be explained straightforwardly from the definition of the OP. Figure 2(b) shows the behaviors of PT as a function of R. We see that the PT is an unimodal function with respect to R and is different from the OP. The rationale behind this phenomenon is that when R is relatively small, the PT is dominated by the term $\log_2(1 + \gamma_{\mathrm{th}})$, when R is large, on the other hand, PT is heavily dependent on OP. Additionally, we observe again that the 2nd scheme is better than the 1st scheme and the mathematical framework agrees with Monte-Carlo simulations.

Full name	Notations	Values [Unit]
Carrier frequency	f_{c}	2.5 [GHz]
Path-loss exponent	χ	3.75
Transmission bandwidth	BW	2 [MHz]
Noise figure	NF	6 [dB]
Expected rate	R	$0 \rightarrow 4$ [bits/s/Hz]
Number of robots	$\mathcal{N}$	4
Transmit power of source robot	P_{S}	$0 \rightarrow 40$ [dBm]
Transmit power of relay robot	P_{R}	$\{10, 20, 30, 40\}$ [dBm]
Channel gain from a to b	$\lvert c_{a,b}\rvert^2$	3

Tab. 1. Simulation parameters.

The behaviors of the OP and PT with respect to the transmit power of the relay robot are given in Fig. 3. It is certain that increasing P_{R} will be beneficial for both metrics that OP will decrease while PT will increase. Moreover, when P_{R} is small, there is a big gap between the two schemes. Nonetheless, when P_{R} is sufficiently large, both schemes achieve the same performance. Interestingly, different from Fig. 2 where OP is an unimodal function with respect to R, OP as a function of P_{R} is a monotonic increasing function. The explanation is the following: when P_{R} is increasing OP in (7), (12) keep decreasing, thus, PT simply goes up with P_{R}.

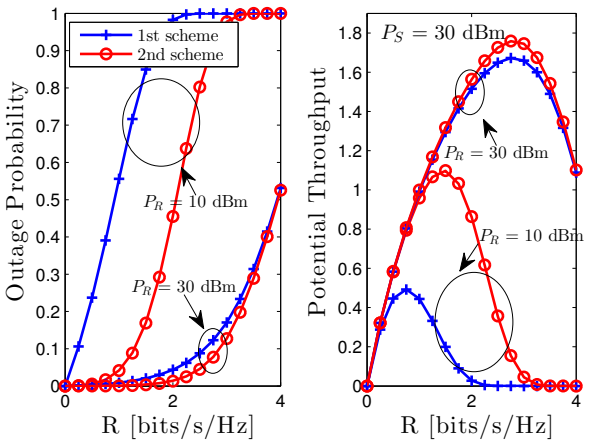

Fig. 2. OP and PT vs. R of two schemes. Solid lines are plotted from (7), (12) and (13). Markers are from Monte-Carlo simulations.

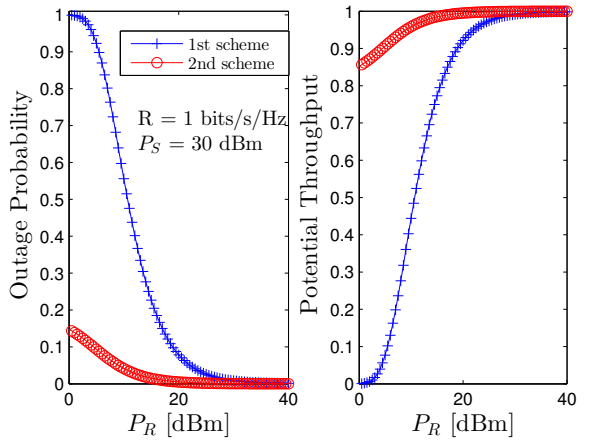

Fig. 3. OP and PT vs. P_{R} of two schemes. Solid lines are plotted from (7), (12) and (13). Markers are from Monte-Carlo simulations.

[1] The Matlab sources of the Monte Carlo simulations are available at: https://drive.google.com/drive/folders/1I5tQp6ToouDePUuwuRWNZBjw8r0O__xk?usp=drive_link

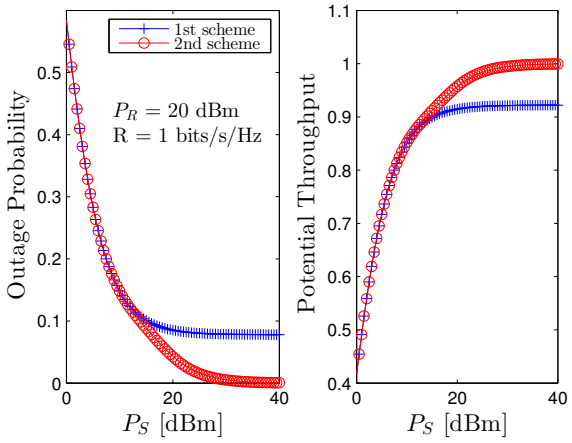

Fig. 4. OP and PT vs. P_S of two schemes. Solid lines are plotted from (7), (12) and (13). Markers are from Monte-Carlo simulations.

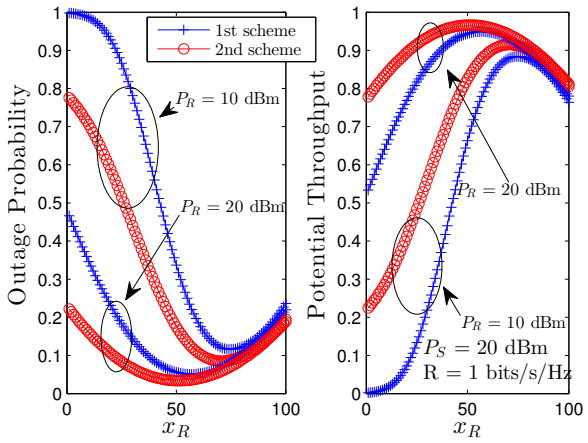

Fig. 5. OP and PT vs. x_R of two schemes. Solid lines are plotted from (7), (12) and (13). Markers are from Monte-Carlo simulations.

The influence of P_S on the performance of OP and PT is given in Fig. 4. We observe that the impact of P_S on the OP and PT is similar to the influence of P_R that raising P_S will decline OP and scale up the PT. However, different from the impact of P_R where the performance of both schemes converges when $P_R \gg 1$, we observe a constant gap between both schemes when $P_S \gg 1$. It can be explained that when P_S goes without bound, under the 1st scheme, the relay robot always decodes error-free signals from the centre robot. Nonetheless, there still exists errors in the transmission from the immediate robot to all terminals unless the transmit power of relay robots approaches infinity too. Thus, a floor exists for this scheme. On the other hand, there is no floor for the 2nd scheme since the transmission from the central robot to the terminals is ideal owing to the infinite transmit power. Interestingly, both schemes achieve the same performance when P_S is small or moderate, e.g., $P_S < 15$ dBm. The rationale behind this phenomenon is that when P_S is small, the relay robot as well as all terminal robots are not able to decode signals from the source, thus, degrading the performance of the whole system. One of the feasible solutions to overcome such constraints is to employ multiple relay robots [18].

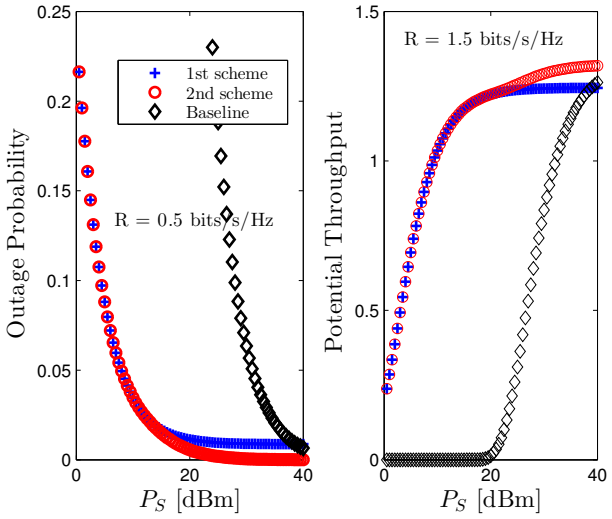

Fig. 6. OP and PT vs. P_S with different values of R. All curves are plotted by Monte-Carlo simulations.

Figure 5 studies the impact of the position of the relay robot, the x-axis of the relay robot x_R, on the performance of both metrics. We see that the system achieves the best performance when the relay robot is located in the middle between the central robot and terminal robots. Moreover, we see that it seems that R locating close to terminal robots provides better performance compared with close to the central node. Additionally, when x_R approaches terminal robots, both schemes almost converge to the same values while x_R closes to the central robot, and we experience a big gap between the two schemes. This figure also confirms again that increasing P_R improves the performance of two metrics regardless of the utilized scheme.

Figure 6 stretches the performance of the OP and PT regarding the P_S of two proposed schemes and the baseline. The curves denoted by 'Baseline' signify that there is only a direct link from the central robot to the terminals. It is certain that without the help from the relay robot the PT of the worst robot is equal to zero when $P_S \leq 20$ dBm while the PT of the two proposed schemes are consistently greater than zeros. Nonetheless, when P_S goes without bounded, the help from the relay becomes minor and the baseline achieves the performance as the 2nd scheme. This can be explained that under the high transmit power of the central robot, all terminals are able to successfully decode the sink's messages. As a result, the proposed solution outperforms the conventional point-to-point communications under the low and moderate of the P_S and has the same performance when $P_S \gg 1$.

5. Conclusions

This paper studied the communication performance of the multi-robot networks where a central robot has information to broadcast to all terminal robots with the help of the relay robot under two scenarios, with and without direct links from the central robot to the terminals. We derived the out-

age probability and potential throughput of the worst robot in the closed-form expression. We provided numerical results to confirm the accuracy of the derived mathematical framework and to identify behaviors of both metrics under some key parameters, including the transmit power of both central and relay robots. Our findings showed that increasing the transmit power at the central robot and/or relay is beneficial for the system and if the immediate robot locates far from the central robot provides better performance compared to the case close to the source robot. This work can be enhanced in several directions. One of the feasible directions is to employ multiple immediate robots to significantly enhance the system performance [18]. Additionally, considering multiple transmit antenna is also a useful solution to boost the system reliability [19]. Besides, considering Fountain codes, massive MIMO and reconfigurable intelligent surfaces are also wise solutions to facilitate the throughput and energy efficiency of the system [20–23].

Acknowledgments

This study was funded by project code MHN2021-01.18 from the Ha Noi Open University.

References

[1] JAWHAR, I., MOHAMED, N., WU, J., et al. Networking of multi-robot systems: Architectures and requirements. *Journal of Sensor and Actuator Networks*, 2018, vol. 7, no. 4, p. 1–16. DOI: 10.3390/jsan7040052

[2] LI, R., XIAO, Y., YANG, P., et al. UAV-aided two-way relaying for wireless communications of intelligent robot swarms. *IEEE Access*, 2020, vol. 8, p. 56141–56150. DOI: 10.1109/ACCESS.2020.2979478

[3] ZHONG, X., ZHOU, Y. Establishing and maintaining wireless communication coverage among multiple mobile robots using a radial basis network controller trained via reinforcement learning. In *IEEE International Conference on Robotics and Biomimetics (ROBIO)*. Shenzhen (China), 2013, p. 1353–1359. DOI: 10.1109/ROBIO.2013.6739653

[4] KRESTOVNIKOV, K., CHERSKIKH, E., SAVELIEV, A. Structure and circuit solution of a bidirectional wireless power transmission system in applied robotics. *Radioengineering*, 2021, vol. 30, no. 1, p. 142–149. DOI: 10.13164/re.2021.0142

[5] ZHANG, Y., LIU, T., ZHANG, H., et al. LEACH-R: LEACH relay with cache strategy for mobile robot swarms. *IEEE Wireless Communications Letters*, 2021, vol. 10, no. 2, p. 406–410. DOI: 10.1109/LWC.2020.3033039

[6] SHARMA, H., RAJESH, M. Design and simulation of WSN for ZigBee based communication in multi-robot system. In *International Conference on Energy, Communication, Data Analytics and Soft Computing (ICECDS)*. Chennai (India), 2017, p. 1353–1355. DOI: 10.1109/ICECDS.2017.8389664

[7] CHUDE-OKONKWO, U. A. K., NUNOO, S., NGAH, R. Time-varying UWB channel model for mobile robot-to-robot communication systems. In *IEEE 11th Malaysia International Conference on Communications (MICC)*. Kuala Lumpur (Malaysia), 2013, p. 1–6. DOI: 10.1109/MICC.2013.6805789

[8] SUGIYAMA, H., TSUJIOKA, T., MURATA, M. Integrated operations of multi-robot rescue system with ad hoc networking. In *1st International Conference on Wireless Communication, Vehicular Technology, Information Theory and Aerospace & Electronic Systems Technology (Wireless VITAE)* . Aalborg (Denmark), 2009, p. 535–539. DOI: 10.1109/WIRELESSVITAE.2009.5172502

[9] NGUYEN, N. P., THANH, T. L., DUONG, Q. T., et al. Secure communications in cognitive underlay networks over Nakagamim channel. *Physical Communication*, 2017, vol. 25, p. 610–618. DOI: 10.1016/j.phycom.2016.05.003

[10] TU, L.-T., DI RENZO, M. On the energy efficiency of heterogeneous cellular networks with renewable energy sources: A stochastic geometry framework. *IEEE Transactions on Wireless Communications*, 2020, vol. 19, no. 10, p. 6752–6770. DOI: 10.1109/TWC.2020.3005618

[11] LIU, J., SHENG, M., LIU, L., et al. Effect of densification on cellular network performance with bounded pathloss model. *IEEE Communications Letters*, 2016, vol. 21, no. 2, p. 346–349. DOI: 10.1109/LCOMM.2016.2615298

[12] DI RENZO, M., TU, L.-T., ZAPPONE, A., et al. A tractable closed-form expression of the coverage probability in Poisson cellular networks. *IEEE Wireless Communications Letters*, 2018, vol. 8, no. 1, p. 249–252. DOI: 10.1109/LWC.2018.2868753

[13] DI RENZO, M., ZAPPONE, A., TU, L.-T., et al. Spectral-energy efficiency pareto front in cellular networks: A stochastic geometry framework. *IEEE Wireless Communications Letters*, 2018, vol. 8, no. 2, p. 424–427. DOI: 10.1109/LWC.2018.2874642

[14] ZHANG, Z., WU, Q., WANG, J. ARQ protocols in cognitive decode-and-forward relay networks: Opportunities gain. *Radioengineering*, 2015, vol. 24, no. 1, p. 54–63. DOI: 10.13164/re.2015.0054

[15] LIU, P., PEROVIC, N. S., SPRINGER, A. The impact of user effects on the performance of dual receive antenna diversity systems in flat Rayleigh fading channels. *Radioengineering*, 2014, vol. 23, no. 1, p. 286–299. ISSN: 1805-9600

[16] CHITRA, M., YASHASWINI, S., DHANASEKARAN, S. Performance analysis of cooperative underlay NOMA-assisted cognitive radio networks. *IEEE Wireless Communications Letters*, 2023, Early Access, p. 1–5. DOI: 10.1109/LWC.2023.3325240

[17] 3RD GENERATION PARTNERSHIP PROJECT (3GPP). *TS 36.101: Evolved Universal Terrestrial Radio Access (E-UTRA); User Equipment (UE) radio transmission and reception (18.3.0 ed.)*. 2023. Cited 2023-10-30. Available at: https://portal.3gpp.org/desktopmodules/Specifications/SpecificationDetails.aspx?specificationId=2411

[18] KESHAVAMURTHY, B., BLISS, M. A., MICHELUSI, N. MAESTRO-X: Distributed orchestration of rotary-wing UAV-relay swarms. *IEEE Transactions on Cognitive Communications and Networking*, 2023, vol. 9, no. 3, p. 794–810. DOI: 10.1109/TCCN.2023.3248859

[19] SELVAM, P. D., VISHVAKSENAN, K. S. Antenna selection and power allocation in massive MIMO. *Radioengineering*, 2019, vol. 28, no. 1, p. 340–346. DOI: 10.13164/re.2019.0340

[20] TRINH, V. C., NGUYEN, C. T., BJÖRNSON, E., et al. Power control in cellular massive MIMO with varying user activity: A deep learning solution. *IEEE Transactions on Wireless Communications*, 2020, vol. 19, no. 9, p. 5732–5748. DOI: 10.1109/TWC.2020.2996368

[21] TRINH, V. C., PAPAZAFEIROPOULOS, A. K., TU, L.-T., et al. Outage probability analysis of IRS-assisted systems under spatially correlated channels. *IEEE Wireless Communications Letters*, 2021, vol. 10, no. 8, p. 1815–1819. DOI: 10.1109/LWC.2021.3082409

[22] TRINH, V. C., TU, L.-T., TRAN, D. H., et al. Controlling smart propagation environments: Long-term versus short-term phase shift optimization. In *IEEE International Conference on Acoustics, Speech and Signal Processing (ICASSP)*. Singapore, 2022, p. 5348–5352. DOI: 10.1109/ICASSP43922.2022.9746584

[23] NGUYEN, N.-L., TU, L.-T., NGUYEN, T. N., et al. Performance on cognitive broadcasting networks employing fountain codes and maximal ratio transmission. *Radioengineering*, 2023, vol. 32, no. 1, p. 1–10. DOI: 10.13164/re.2023.0001

About the Authors ...

Van Son NGUYEN received a B.E. degree in Electrical Engineering and an M.S. degree in Electronics and Telecommunications Engineering from Hanoi Open University, Hanoi, Vietnam. He is currently a Lecturer with the Faculty of Electrical and Electronic Engineering, at Hanoi Open University. His research interests include signal processing in B5G/6G systems and ML/AI applications in big data processing.

Trinh Van CHIEN received the B.S. degree in Electronics and Telecommunications from Hanoi University of Science and Technology (HUST), Vietnam, in 2012. He then received the M.S. degree in Electrical and Computer Engineering from Sungkyunkwan University (SKKU), Korea, in 2014 and the Ph.D. degree in Communication Systems from Linkoping University (LiU), Sweden, in 2020. He was a research associate at the University of Luxembourg. He is now with the School of Information and Communication Technology (SoICT), Hanoi University of Science and Technology (HUST), Vietnam.

Dang Khanh HOA graduated from Hanoi University of Science and Technology in 2002, majoring in Electronics and Telecommunications. In 2005, he graduated with a master's degree in Electronic Engineering from Hanoi University of Science and Technology. In 2020, he was awarded a doctorate in Electronic Engineering at the School of Electrical and Electronics Engineering, Hanoi University of Science and Technology. His research focuses mainly on computer vision, applied to wheeled robot control.

Do Dinh HUNG received a Ph.D. in Telecommunications Engineering in 2023. Currently working at Hanoi Open University. Research field: Signal processing techniques and radio and wire communications and hydroacoustic information transmission using single or multiple antenna transceiver systems.

Hoai Giang NGUYEN received the B.S. degree in Technical Informatics from the Budapest University of Technology and Economics, Hungary, in 1999, and the Ph.D. degree in Electronic Engineering from the Hanoi University of Science and Technology, Hanoi, Vietnam, in 2009. He is currently the Dean of the Faculty of Electrical and Electronic Engineering, Hanoi Open University, Vietnam. His research interests include the application of technology in the fields of education, break training, and health.

Chi Quynh LE received the B.E. degree in Telecommunications Engineering from Hanoi University of Science and Technology, Hanoi, Vietnam in 1967. In 1987, he was awarded a doctorate in Electronic Engineering at the School of Electrical and Electronics Engineering, Hanoi University of Science and Technology. His research interests include signal processing in B5G/6G systems and ML/AI applications in big data processing

Lam-Thanh TU (* Corresponding author, email: tulamthanh@tdtu.edu.vn) received the Ph.D. degree from the University of Paris Sud, Paris-Saclay University, France, in 2018. Currently, he is with the Faculty of Electrical and Electronics Engineering, Ton Duc Thang University, Vietnam. He was a recipient of the 2017 IEEE SigTelCom and the 2022 RICE Best Paper Award. His research interests include stochastic geometry, LoRa networks, reconfigurable intelligent surfaces, covert communications, and artificial intelligence applications for wireless communications.

Appendix A: Proof of Equation (12)

In this section, we are going to derive the OP under the 2nd scheme. Let us start with rewriting (12) as

$$\begin{aligned}\mathrm{OP}^{\mathrm{C2}} &= \int_{x=0}^{\infty} \mathrm{OP}_X^{\mathrm{C2}}(R;x)\, f_{X=|c_{\mathrm{S,R}}|^2}(x)\,\mathrm{d}x \\ &= \int_{x=0}^{\infty} \left[1 - \prod_{n=1}^{N} \overline{F}_{\gamma_n^{\mathrm{e2e,C2}}\left|X\right.}(\gamma_{\mathrm{th}})\right] \frac{1}{\alpha_{|c_{\mathrm{S,R}}|^2}} \exp\left(-\frac{x}{\alpha_{|c_{\mathrm{S,R}}|^2}}\right)\mathrm{d}x\end{aligned} \tag{A1}$$

To (A1), let us first explicitly represent the term $\overline{F}_{\gamma_n^{\mathrm{e2e,C2}}\left|X\right.}(\gamma_{\mathrm{th}})$ as follows

$$\begin{aligned}\overline{F}_{\gamma_n^{\mathrm{e2e,C2}}\left|X\right.}(\gamma_{\mathrm{th}}) &= 1 - \left(1 - \exp\left(-\frac{\gamma_{\mathrm{th}} l_{\mathrm{S},n}\sigma^2}{P_{\mathrm{S}}\alpha_{|c_{\mathrm{S},n}|^2}}\right)\right) \\ &\times \left[1 - \exp\left(-\gamma_{\mathrm{th}}\frac{P_{\mathrm{S}} l_{\mathrm{R},n}}{\alpha_{|c_{\mathrm{R},n}|^2} P_{\mathrm{R}} l_{\mathrm{S,R}}}\frac{l_{\mathrm{S,R}}\sigma^2}{P_{\mathrm{S}}}\right)\mathrm{H}\left(x - \gamma_{\mathrm{th}}\frac{l_{\mathrm{S,R}}\sigma^2}{P_{\mathrm{S}}}\right)\right] \\ &= 1 - (1 - A_n)\left[1 - \exp\left(-\gamma_{\mathrm{th}}\frac{l_{\mathrm{R},n}\sigma^2}{\alpha_{|c_{\mathrm{R},n}|^2} P_{\mathrm{R}}}\right)\mathrm{H}\left(x - \gamma_{\mathrm{th}}\frac{l_{\mathrm{S,R}}\sigma^2}{P_{\mathrm{S}}}\right)\right] \\ &= A_n + (1 - A_n)\exp\left(-\gamma_{\mathrm{th}}\frac{l_{\mathrm{R},n}\sigma^2}{\alpha_{|c_{\mathrm{R},n}|^2} P_{\mathrm{R}}}\right)\mathrm{H}\left(x - \gamma_{\mathrm{th}}\frac{l_{\mathrm{S,R}}\sigma^2}{P_{\mathrm{S}}}\right) \\ &= A_n + B_n \mathrm{H}\left(x - \gamma_{\mathrm{th}}\frac{l_{\mathrm{S,R}}\sigma^2}{P_{\mathrm{S}}}\right)\end{aligned} \tag{A2}$$

where A_n, B_n are defined in (12). Next, we re-formulate the term $\prod_{n=1}^{N} \overline{F}_{\gamma_n^{\mathrm{e2e,C2}}\left|X\right.}(\gamma_{\mathrm{th}})$ as follows:

$$\prod_{n=1}^{N}\left(A_n + B_n H\left(x-\gamma_{\text{th}}\frac{l_{\text{S,R}}\sigma^2}{P_{\text{S}}}\right)\right) = \left(\prod_{n=1}^{N} A_n\right) \times \left(\prod_{n=1}^{N}\left[1 + C_n H\left(x-\gamma_{\text{th}}\frac{l_{\text{S,R}}\sigma^2}{P_{\text{S}}}\right)\right]\right) \quad \text{(A3)}$$

where $C_n = B_n/A_n$. Finally, substituting (A3) into (A1), we obtain (12) as below and close the proof here.

$$\begin{aligned}
\text{OP}^{\text{C2}} &= \int_{x=0}^{\infty} \frac{1}{\alpha_{|c_{\text{S,R}}|^2}} \exp\left(-\frac{x}{\alpha_{|c_{\text{S,R}}|^2}}\right)\left[1-\left(\prod_{n=1}^{N} A_n\right)\right. \\
&\left.\times\left(\prod_{n=1}^{N}\left[1+C_n \text{H}\left(x-\gamma_{\text{th}}\frac{l_{\text{S,R}}\sigma^2}{P_{\text{S}}}\right)\right]\right)\right] \text{d}x \\
&= 1-\left(\prod_{n=1}^{N} A_n\right)\frac{1}{\alpha_{|c_{\text{S,R}}|^2}}\int_{x=0}^{\infty}\exp\left(-\frac{x}{\alpha_{|c_{\text{S,R}}|^2}}\right) \\
&\times\left(\prod_{n=1}^{N}\left[1+C_n \text{H}\left(x-\gamma_{\text{th}}\frac{l_{\text{S,R}}\sigma^2}{P_{\text{S}}}\right)\right]\right)\text{d}x \\
&= 1-\left(\prod_{n=1}^{N} A_n\right)\frac{1}{\alpha_{|c_{\text{S,R}}|^2}}\int_{x=0}^{\infty}\left[\int_{x=0}^{\gamma_{\text{th}}\frac{l_{\text{S,R}}\sigma^2}{P_{\text{S}}}}\exp\left(-\frac{x}{\alpha_{|c_{\text{S,R}}|^2}}\right)\text{d}x\right. \\
&\left.+\int_{x=\gamma_{\text{th}}\frac{l_{\text{S,R}}\sigma^2}{P_{\text{S}}}}^{\infty}\left(\prod_{n=1}^{N}[1+C_n]\right)\exp\left(-\frac{x}{\alpha_{|c_{\text{S,R}}|^2}}\right)\text{d}x\right] \\
&= 1-\left(\prod_{n=1}^{N} A_n\right)\left[\left(\prod_{n=1}^{N}[1+C_n]\right)\exp\left(-\gamma_{\text{th}}\frac{l_{\text{S,R}}\sigma^2}{P_{\text{S}}\alpha_{|c_{\text{S,R}}|^2}}\right)\right. \\
&\left.+\frac{1}{\alpha_{|c_{\text{S,R}}|^2}}\left(1-\exp\left(-\gamma_{\text{th}}\frac{l_{\text{S,R}}\sigma^2}{P_{\text{S}}\alpha_{|c_{\text{S,R}}|^2}}\right)\right)\right].
\end{aligned} \quad \text{(A4)}$$

We, therefore, conclude the proof.